



## Some studies on hard turning of AISI 4340 steel using multilayer coated carbide tool

R. Suresh <sup>a</sup>, S. Basavarajappa <sup>b,\*</sup>, G.L. Samuel <sup>c</sup>

<sup>a</sup> Department of Mechanical Engineering, Canara Engineering College, Mangalore 574 219, Karnataka, India

<sup>b</sup> Department of Studies in Mechanical Engineering, University BDT College of Engineering, Davangere 577 004, Karnataka, India

<sup>c</sup> Department of Mechanical Engineering, Indian Institute Technology Madras, Chennai 600 036, Tamil Nadu, India

### ARTICLE INFO

#### Article history:

Received 28 October 2011

Received in revised form 25 February 2012

Accepted 21 March 2012

Available online 30 March 2012

#### Keywords:

Hard turning

Coated carbide

Taguchi technique

ANOVA

### ABSTRACT

Hard turning with multilayer coated carbide tool has several benefits over grinding process such as, reduction of processing costs, increased productivities and improved material properties. The objective was to establish a correlation between cutting parameters such as cutting speed, feed rate and depth of cut with machining force, power, specific cutting force, tool wear and surface roughness on work piece. In the present study, performance of multilayer hard coatings (TiC/TiCN/Al<sub>2</sub>O<sub>3</sub>) on cemented carbide substrate using chemical vapor deposition (CVD) for machining of hardened AISI 4340 steel was evaluated. An attempt has been made to analyze the effects of process parameters on machinability aspects using Taguchi technique. Response surface plots are generated for the study of interaction effects of cutting conditions on machinability factors. The correlations were established by multiple linear regression models. The linear regression models were validated using confirmation tests. The analysis of the result revealed that, the optimal combination of low feed rate and low depth of cut with high cutting speed is beneficial for reducing machining force. Higher values of feed rates are necessary to minimize the specific cutting force. The machining power and cutting tool wear increases almost linearly with increase in cutting speed and feed rate. The combination of low feed rate and high cutting speed is necessary for minimizing the surface roughness. Abrasion was the principle wear mechanism observed at all the cutting conditions.

© 2012 Elsevier Ltd. All rights reserved.

### 1. Introduction

Modern machine tools, with increased dynamic performance, stiffness and power, require cutting tools with highly improved properties, in particular on their surfaces. The fact holds good even during machining of difficult to cut alloy steels. Correlation between chemical, physical and mechanical characteristics of cutting tools surface and their performances in cutting operations is therefore a key issue for both tool manufacturers and users [1].

Various studies have been conducted to investigate the performance of coated carbide, ceramic and CBN tools in

the machining of various hard materials. Cutting forces, tool wear and surface roughness are the major factors considered while machining of ferrous alloys in their hardened state. Cutting force is the important technological parameter to control in machining process. It is the background for evaluation of the necessary power for machining, dimensioning of machine tool components and tool body. It influences machining system stability. In hard turning, cutting forces have been found to be influenced by a number of factors such as cutting conditions, cutting time and work piece hardness [2,3].

Nakayama et al. [4] indicated that cutting forces in the machining of hard materials are not necessarily high compared with those of soft materials. A high shear angle and the formation of saw-toothed chips due to poor ductility

\* Corresponding author. Tel./fax: +91 8192 2224567.

E-mail address: [basavarajapps@yahoo.com](mailto:basavarajapps@yahoo.com) (S. Basavarajappa).

### Nomenclature

$V_c$	cutting speed (m/min)	$P_m$	machining power (kW)
$f$	feed rate (mm/rev)	$K_s$	specific cutting force (MPa)
$d$	depth of cut (mm)	$VB_{max}$	tool flank wear (mm)
$F_c$	cutting force (N)	$R_a$	surface roughness ( $\mu\text{m}$ )
$F_f$	feed force (N)		
$F_t$	thrust force (N)		
$F_m$	machining force (N)		

reduce the forces despite the high strength of hard materials. In addition, tool wear due to abrasion in the machining of hard materials increases the cutting forces, especially the thrust force. Luo et al. [5] have investigated the relationship between hardness and cutting forces during turning AISI 4340 steel hardened from 29 to 57 HRC using mixed alumina tools. The results suggest that an increase of 48% in hardness leads to an increase in cutting forces from 30% to 80%. It is reported that for work material hardness values between 30 and 50 HRC, continuous chips were formed and the cutting force components were reduced. However, when the workpiece hardness increased above 50 HRC, segmented chips were observed and the cutting force showed a sudden increase.

Tool geometry is another important factor affecting machining process, especially the feed force and thrust force components [6]. When cutting hardened steels, the use of chamfered edges and negative rake angle and inclination angles helps to increase the machining forces. In addition to that the use of large nose radius together with low depth of cut leads to low true side cutting edge angle values (irrespective of tool holder geometry), thus resulting in high thrust forces. On the other hand, large nose radius and cutting edge angle values may improve the surface finish of the machined part provided tool vibration can be controlled [7].

Machining conditions greatly influences the machining of hardened steels. Li and Hossan [8] numerical simulations are compared to experimental results, Cutting forces and feed forces were determined in the numerical simulations technique. Among process parameters, cutter geometry and work piece hardness, the feed rate has the most significant effect on cutting and feed forces. With same cutting conditions, turning AISI 4340 gets the highest cutting force while turning AISI 52100 has the highest feed force and turning AISI D2 gets the lowest cutting force and feed force. The feed force appears to be a larger force component than the cutting force in the hard turning. Cutting force and feed force increase with increasing feed, tool edge radius, negative rake angle, and work piece hardness.

The majority of hard turning concerned with composition, thermal, wear characteristics of cutting tools, effect of work material hardness, tool geometry and influence of cutting conditions on surface integrity of the finish machined parts [9]. Since hard turning demands a strong and prudent tool cutting edge, nose design with proper edge preparation becomes crucial to provide high edge strength as well as to attain favorable surface roughness and subsurface residual stresses. Performance of coated carbides,

ceramic and CBN cutting tools and the quality of the surfaces machined are highly dependent on the cutting conditions, i.e. cutting speed, feed, depth of cut and tool geometry [10].

Yang and Tarn [11] used the Taguchi method to find the optimal cutting parameters for turning operation. An orthogonal array (OA) and the analysis of variance (ANOVA) are employed to investigate the cutting characteristics using cemented carbide tools. Davim and Figueira [12] investigated the machinability of AISI D2 tool steel using experimental and statistical techniques. Hard turning operation was performed on material having hardness 60 HRC, the tests are conducted by using cutting speed, feed rate and time as main parameters and analysis was done based on the responses. The influence of cutting parameters under flank wear, specific cutting force and surface roughness on machinability evaluation in turning with ceramic tools using ANOVA is presented. Ozel et al. [13] conducted a set of ANOVA and performed a detailed experimental investigation on the surface roughness and cutting forces in the finish hard turning of AISI H13 steel. Their results indicated that the effects of work piece hardness, cutting edge geometry, feed rate and cutting speed on surface roughness are statistically significant.

Advances in coating technology have resulted in a new generation of high performance coated carbide tools exhibiting improved properties such as fracture strength, toughness, thermal shock resistance, wear resistance and hardness. Surfaces of cemented carbide cutting tools need to be abrasion resistant, hard and chemically inert to prevent the tool and the work material from interacting chemically with each other during machining. Coated carbides are basically a cemented carbide insert material coated with one or more thin layers of wear resistant material such as titanium carbide (TiC), Titanium nitride (TiN) and aluminum oxide ( $\text{Al}_2\text{O}_3$ ) [14]. It is well known that thin (0.1 to 30  $\mu\text{m}$ ), hard (>2500 VHN) coatings can reduce tool wear and improve tool life and also productivity [15].

Yigit et al. [16] investigated that a multilayer TiCN/TiC/ $\text{Al}_2\text{O}_3$ /TiN coating with an external TiN layer is the best-suited tool for minimizing flank wear and surface roughness in hard turning. Aneiro et al. [17] have studied the turning of hardened steel using TiCN/ $\text{Al}_2\text{O}_3$ /TiN coated carbide tool and PCBN tools during turning of hardened steel. They observed that better tool life could be achieved using PCBN tool, but cost of the PCBN tool is as twice as that of the coated carbide tool. Machining medium hardened steels with TiCN/ $\text{Al}_2\text{O}_3$ /TiN inserts tend to be more productive. The relatively good performance of coated carbide

tools in machining hardened steel relied on the coating combination of layers. Knuttsson et al. [18] have stated that TiAlN/TiN multilayer has exhibited better wear resistance, attributed to the multilayer hardening effects and enhanced thermal stability.

Yigit et al. [19] have found that multilayer coating on carbide substrate enhances the tool life performance when compared with uncoated carbide tools. Decrease in cutting force was obtained with high temperature chemical vapor deposition (HTCVD) multilayer carbide tools compared to uncoated carbide tool. Ciftci [20] investigated the dry turning of austenitic stainless steels using CVD multilayer-coated cemented carbide tools. It was reported that TiN coating has a lower coefficient of friction than  $Al_2O_3$  coating. Bouzakis et al. [21] stated that film failure after the coating fracture initiation was less intense in case of multilayer coating and can be attributed to the deceleration of potential cracks propagation within the layered TiN/TiAlN structure. They reported that by applying the multilayer coatings tool life could be improved.

The fundamental idea behind the introduction of multilayer coated carbide tool is to take advantage of higher cutting speed in order to achieve increased material removal rates during machining of hardened alloys. Recently many researchers have focused on performance of multilayer coated carbide tools for machining of hard materials. Higher cutting speed process and reduce in friction between tool and work piece material are the major parameters considered in previous studies to produce better surface finish [22].

The literature reveals that, limited literatures are available on the multilayer, multimaterial cutting tools in turning of hardened AISI 4340 steel. Further, there is need to present models which correlates the cutting parameters with the machinability characteristics during hard turning. Hence in the present study, the attention is paid towards the multilayer multimaterial coated cemented carbide tool and its performance during turning of hardened AISI 4340 steel. Besides main objective of the study was to investigate the influence of cutting parameters such as feed rate, depth of cut, cutting speed and their interaction on machinability characteristics such as machining force, specific cutting force, power required, tool wear and surface roughness and to correlate them by presenting statistical models. The Taguchi design approach is utilized for planning experiments and ANOVA is employed for analysis.

## 2. Experimental procedure

### 2.1. Workpiece material

In this study, the chosen workpiece material was high strength low alloy AISI 4340 steel in the form of round bars having 100 mm diameter and 400 mm length. The workpiece was through-hardened followed by tempering to achieve 48 HRC. In order to assure the required stiffness of chuck/workpiece/cutting system, the ratio of cylindrical turning length to the initial diameter of workpiece was approximately kept as 4. The steel investigated here is widely employed for the production of automobile and machine tool parts such as axle shafts, main shafts, spindles,

gears, power transmission gears and couplings. The chemical composition of AISI 4340 steel was evaluated using an optical emission spectrometer and the obtained chemical composition is given in Table 1.

### 2.2. Cutting tool and tool geometry

The coated carbide inserts of ISO geometry CNMG 120408 were used throughout the investigation. The inserts have a multilayer CVD coating (TiN/TiCN/ $Al_2O_3$ ) on cemented carbide substrate. The CVD coating consisted of a thick, moderate temperature chemical vapor deposition (MT CVD) of TiN for heat resistance and with low coefficient of friction, TiCN for wear resistance and thermal stability and  $Al_2O_3$  for high temperature/hot hardness and crater wear resistance. The combined top coating and gradient substrate provided extremely good behavior during dry machining. The 'PCLNL2525 M12' (ISO) type tool holder was employed with tool geometry as follows: including angles =  $80^\circ$ , back rake angle =  $-6^\circ$ , clearance angle =  $5^\circ$  and approach angle =  $95^\circ$ . The geometry of the tool and order of multilayer are shown in Fig. 1.

### 2.3. Planning of experiments

Taguchi's technique has been used widely in engineering analysis and is a robust design. The Taguchi technique consists of plan of experiments with the objective of acquiring data in a controlled way. After the completion of the experiment the data from all the experiments in the set are analyzed to determine the effect of various parameters. Conducting the experiments in terms of orthogonal array allows the effects of several parameters to be determined efficiently. The treatment of the experimental results is based on the analysis of average and the analysis of variance [23–25].

In the present investigation, three levels are defined for each of the identified factors as illustrated and shown in Table 2. Cutting parameters are selected based on the hardness of work piece material, and chemical composition and guidelines by the cutting tool manufacturer. Taguchi's  $L-27(3^{13})$  orthogonal array was selected for plan of experiments and is shown in Table 3.

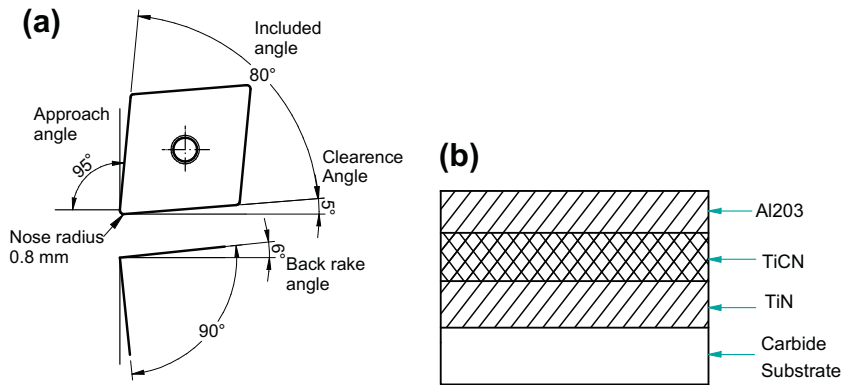
### 2.4. Experimental details

The dry turning experiments were performed on hardened AISI 4340 steel material using coated carbide inserts. Computer numerically controlled (CNC) lathe was employed to conduct the experiments. The lathe is equipped with 22 kw spindle power and a maximum spindle speed of 5000 rpm. Axial and radial run out was checked on the machine and was within the acceptable limit of error. During the machining tests, the cutting force ( $F_c$ ), radial force ( $F_r$ ) and feed force ( $F_f$ ) were measured using a piezo-electric dynamometer (Kistler model 9263A) which was connected to charged amplifiers and a personal computer through an analog to digital converter card. To obtain and record the force data, data acquisition software was used. Cutting forces and their amplitudes were measured with an accuracy of  $\pm 0.012$  N,  $\pm 0.010$  N and  $\pm 0.020$  N, for the  $F_c$ ,  $F_r$  and

**Table 1**

The chemical composition of AISI 4340 steel in percentage by weight.

C	Si	Mn	P	S	Cr	Ni	Mo	Fe
0.382	0.228	0.609	0.026	0.022	0.995	1.514	0.226	95.998

**Fig. 1.** (a) Insert with tool geometry and (b) order of multilayer coating.**Table 2**

Factors and levels used in the experiments.

Factors	Symbol	Level 1	Level 2	Level 3
Cutting speed (m/min)	$V_c$	140	200	260
Feed rate (mm/rev)	$f$	0.10	0.18	0.26
Depth of cut (mm)	$d$	0.60	0.80	1.0

$F_f$ ; constituents of the resultant force, respectively. The photographs of the experimental setup with measurement of the cutting forces by piezoelectric dynamometer and the charge amplifiers with PC based data acquisition system are shown in Fig. 2. The steady state force condition was maintained as shown in Fig. 3.

In each experiment a fresh cutting tool was used for fixed cutting time of 4.0 min and the experiments were repeated twice at each condition in order to keep experimental error at a minimum. After the trials the tools were cleaned in an HCl solution and acetone in order to remove steel residuals adhered to the rake and flank face of the cutting tools. The width of flank wear was measured using optical microscope connected to a digital camera and computer. The surface roughness values were measured immediately after the turning process at five different locations on work piece by using surface roughness tester. The average of five roughness values was taken as an arithmetic surface roughness ( $R_a$ ).

### 3. Experimental results and discussion

The plan of tests was developed with the aim of relating the influence of the cutting speed, feed rate and depth of cut with machinability parameters. The statistical treatment of the data was made in two phases. The first phase was concerned with the ANOVA and the effect of the each factor and interactions. In order to determine the interaction effects of turning process parameters on machining force ( $F_m$ ), specific cutting force ( $K_s$ ), power ( $P_m$ ), tool wear

( $VB_{max}$ ) and surface roughness ( $R_a$ ), the response surface plots were generated considering two parameters at a time while third parameters is kept at constant.

The second phase allowed us to obtain the correlations between the parameters by multiple linear regressions. The outputs to be studied are machining force ( $F_m$ ), specific cutting force ( $K_s$ ); machining power ( $P_m$ ), tool wear ( $VB_{max}$ ) and surface roughness ( $R_a$ ). Trials were run twice and an average value was considered for analysis as shown in Table 3. The measured force components are represented with a mean machining force, which are calculated by using the equation shown in Eqs. (1)–(3).

$$F_m = \sqrt{(F_c^2 + F_f^2 + F_t^2)} \quad (1)$$

$$P_m = F_c V_c, \quad (2)$$

$$K_s = F_c / (f \times d) \quad (3)$$

#### 3.1. Analysis of variance results

ANOVA can be useful for determining influence of any given input parameters from a series of experimental results by design of experiments for machining process and it can be used to interpret experimental data. The obtained results are analyzed using Minitab-16, statistical analysis software which is widely used in many engineering applications. The ANOVA table consists of sum of squares and degrees of freedom. The mean square is the ratio of sum of squares to degrees of freedom and F-ratio is the ratio of mean square to the mean square of the experimental error. As per ANOVA, the calculated value of Test-F of developed model should be more than F-table for the model to be adequate for a specified confidence interval.

Tables 4–8 illustrate the results of ANOVA with the machining force ( $F_m$ ), specific cutting force ( $K_s$ ), the power ( $P_m$ ) required for performing the machining operation, tool

**Table 3**  
Experimental data for hardened AISI 4340 steel machining with coated carbide tool.

Trial No.	Vc (m/min)	F (mm/rev)	D (mm)	Machining force, $F_m$ (N)				Specific cutting force, $K_s$ (MPa)				Machining power, $P_m$ (kW)				Tool wear, $VB_{max}$ (mm)				Surface roughness, $R_a$ ( $\mu$ m)							
				R1		R2		Avg.		S/N		R1		R2		Avg.		S/N (dB)		R1		R2		Avg.		S/N (dB)	
1	140	0.1	0.6	440	444	442.0	-52.91	3890.0	3933.34	3911.67	-71.85	0.40	0.35	0.375	8.52	0.05	0.044	0.047	26.56	0.60	0.54	0.57	4.81				
2	140	0.1	0.8	488	495	491.5	-53.83	3630.0	3687.50	3658.75	-71.27	0.50	0.45	0.475	6.47	0.06	0.052	0.056	25.04	0.66	0.58	0.62	4.22				
3	140	0.1	1.0	546	550	548.0	-54.78	3410.0	3430.00	3420.00	-70.68	0.55	0.50	0.525	5.60	0.07	0.062	0.066	23.61	0.74	0.64	0.69	3.16				
4	140	0.18	0.6	480	486	483.0	-53.68	3220.0	3240.75	3230.38	-70.19	0.60	0.60	0.600	4.44	0.066	0.058	0.062	24.15	1.20	1.12	1.16	-1.29				
5	140	0.18	0.8	602	600	601.0	-55.58	3142.0	3125.00	3133.50	-69.92	0.65	0.70	0.675	3.41	0.075	0.065	0.07	23.10	1.35	1.30	1.33	-2.44				
6	140	0.18	1.0	753	750	751.5	-57.52	3077.8	3066.67	3072.24	-69.75	0.70	0.75	0.725	2.79	0.09	0.084	0.087	21.21	1.40	1.30	1.35	-2.61				
7	140	0.26	0.6	630	628	629.0	-55.97	3148.0	3141.03	3144.52	-69.95	0.80	0.90	0.850	1.41	0.08	0.070	0.075	22.50	2.00	1.84	1.92	-5.69				
8	140	0.26	0.8	734	740	737.0	-57.35	2980.0	2990.38	2985.19	-69.50	0.95	1.05	1.00	0.00	0.09	0.090	0.09	20.92	2.10	2.00	2.05	-6.24				
9	140	0.26	1.0	995	998	996.5	-59.97	2842.0	2846.16	2844.08	-69.08	1.10	1.00	1.05	-0.42	0.11	0.100	0.105	19.58	2.25	1.18	1.72	-4.69				
10	200	0.1	0.6	385	390	387.5	-51.77	3745.0	3800.00	3772.50	-71.53	1.00	0.90	0.950	0.45	0.08	0.080	0.08	21.94	0.46	0.40	0.43	7.43				
11	200	0.1	0.8	415	422	418.5	-52.43	3510.0	3550.00	3530.00	-70.96	1.05	1.00	1.025	-0.21	0.10	0.090	0.095	20.45	0.55	0.45	0.5	5.93				
12	200	0.1	1.0	513	515	514.0	-54.22	3325.0	3350.00	3337.50	-70.47	1.20	1.10	1.150	-1.21	0.11	0.110	0.11	19.17	0.60	0.54	0.57	4.81				
13	200	0.18	0.6	462	455	458.5	-53.23	3152.0	3111.12	3131.56	-69.92	1.10	1.10	1.100	-0.83	0.11	0.102	0.106	19.49	0.85	0.75	0.80	1.94				
14	200	0.18	0.8	580	578	579.0	-55.25	2916.7	2902.77	2909.74	-69.28	1.25	1.20	1.225	-1.76	0.12	0.11	0.115	18.79	0.96	0.84	0.90	0.87				
15	200	0.18	1.0	704	700	702.0	-56.93	2788.9	2777.78	2783.34	-68.89	1.50	1.36	1.430	-3.11	0.13	0.118	0.124	18.13	1.05	1.0	1.03	-0.30				
16	200	0.26	0.6	554	552	553.0	-54.85	2946.0	2935.90	2940.95	-69.37	1.60	1.55	1.575	-3.95	0.15	0.140	0.145	16.77	1.50	1.5	1.50	-3.52				
17	200	0.26	0.8	714	708	711.0	-57.04	2782.0	2764.42	2773.21	-68.86	1.70	1.60	1.65	-4.35	0.17	0.164	0.167	15.55	1.70	1.64	1.67	-4.48				
18	200	0.26	1.0	865	850	857.5	-58.66	2650.0	2634.62	2642.31	-68.44	1.90	1.80	1.85	-5.34	0.19	0.180	0.185	14.66	1.80	1.74	1.77	-4.96				
19	260	0.1	0.6	365	360	362.5	-51.19	3540.0	3500.00	3520.00	-70.93	1.60	1.70	1.65	-4.35	0.15	0.150	0.15	16.48	0.32	0.28	0.30	10.46				
20	260	0.1	0.8	390	386	388.0	-51.78	3387.0	3337.50	3362.25	-70.53	1.80	1.70	1.75	-4.86	0.17	0.160	0.165	15.65	0.45	0.37	0.41	7.85				
21	260	0.1	1.0	480	472	476.0	-53.55	3205.0	3160.00	3182.5	-70.06	1.90	1.84	1.87	-5.44	0.19	0.180	0.185	14.66	0.60	0.52	0.56	5.04				
22	260	0.18	0.6	436	430	433.0	-52.73	3070.0	3055.56	3062.78	-69.72	1.80	1.72	1.76	-4.91	0.17	0.164	0.167	15.55	0.70	0.6	0.65	3.74				
23	260	0.18	0.8	560	565	562.5	-55.00	2777.8	2805.56	2791.68	-68.92	2.00	1.96	1.98	-5.93	0.19	0.180	0.185	14.66	0.88	0.76	0.82	1.72				
24	260	0.18	1.0	685	680	682.5	-56.68	2700.0	2683.34	2691.67	-68.60	2.20	2.10	2.15	-6.65	0.20	0.200	0.2	13.98	0.95	0.85	0.90	0.92				
25	260	0.26	0.6	515	520	517.5	-54.28	2740.0	2756.41	2748.21	-68.78	2.30	2.20	2.25	-7.04	0.24	0.230	0.235	12.58	1.30	1.22	1.26	-2.01				
26	260	0.26	0.8	650	646	648.0	-56.23	2610.6	2596.16	2603.38	-68.31	2.50	2.42	2.46	-7.82	0.28	0.270	0.275	11.21	1.40	1.34	1.37	-2.73				
27	260	0.26	1.0	745	746	745.5	-57.45	2496.2	2500.00	2498.10	-67.95	3.00	3.10	3.05	-9.69	0.32	0.310	0.315	10.03	1.60	1.48	1.54	-3.75				

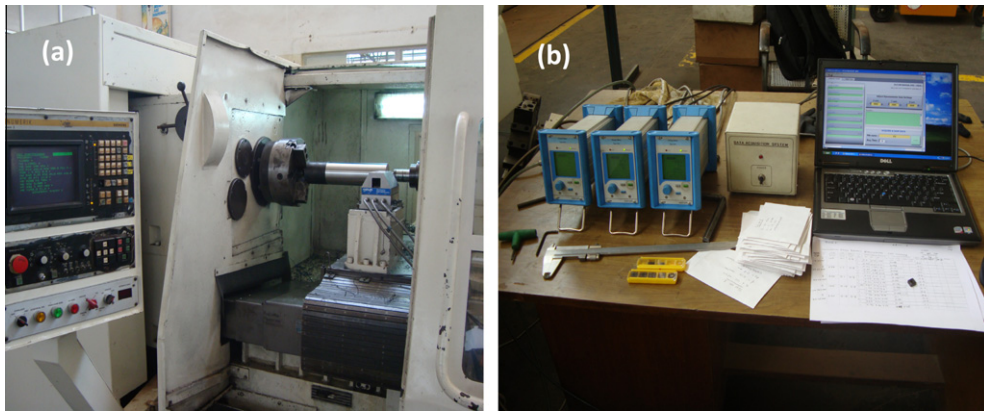


Fig. 2. (a) Experimental setup with measurement of the cutting forces by piezoelectric dynamometer, and (b) charge amplifiers and PC based data acquisition system.

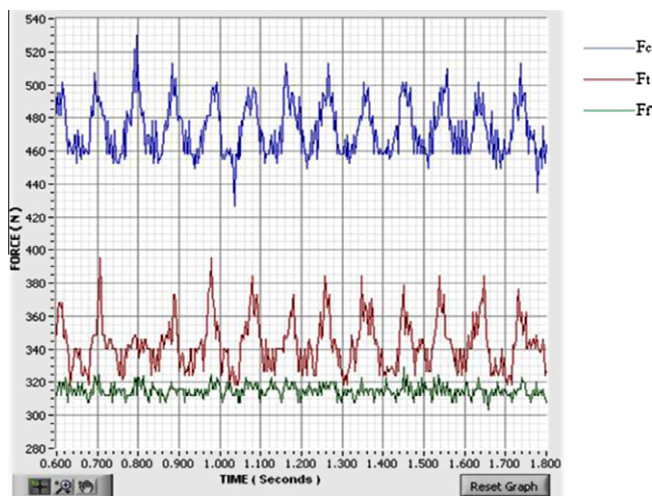


Fig. 3. Example of cutting forces for hardened AISI 4340 steel with coated carbide tool at  $V_c = 200$  m/min,  $f = 0.18$  mm/rev and  $d = 1.0$  mm.

Table 4  
ANOVA results for machining force ( $F_m$ ).

Factors	SS	D.o.f	Variance	Test F	$F_{table}$	P (%)
$f$	69.91	2	34.96	349.60	8.65 <sup>a</sup>	53.38
$d$	47.26	2	23.63	236.30	8.65 <sup>a</sup>	36.04
$V_c$	9.01	2	4.50	45.00	8.65 <sup>a</sup>	6.75
$f \times d$	2.63	4	0.66	6.60	3.84 <sup>b</sup>	1.71
$V_c \times f$	0.92	4	0.23	2.30	1.66 <sup>c</sup>	0.40
$V_c \times d$	0.09	4	0.023	0.23	–	–
Error	0.79	8	0.10			1.72
Total	130.61	26				100.00

SS = Sum of squares; d.o.f = degree of freedom; P = percentage of contribution.

- <sup>a</sup> 99% Confidence.
- <sup>b</sup> 95% Confidence.
- <sup>c</sup> 75% Confidence.

wear ( $VB_{max}$ ) and surface roughness ( $R_a$ ) in work piece, respectively. The last column of the tables shows the percentage of contribution (P) of the each factor on the total variation indicating, the degree of their influence on the result.

Table 5  
ANOVA results for specific cutting force ( $K_s$ ).

Factors	SS	D.o.f	Variance	Test F	$F_{table}$	P (%)
$f$	18.88	2	9.44	502.13	8.65 <sup>a</sup>	70.55
$d$	3.79	2	1.895	100.80	8.65 <sup>a</sup>	14.05
$V_c$	3.62	2	1.81	96.28	8.65 <sup>a</sup>	13.42
$V_c \times f$	0.19	4	0.0475	2.53	1.66 <sup>b</sup>	0.43
$V_c \times d$	0.03	4	0.0075	0.40	–	–
$f \times d$	0.05	4	0.0125	0.67	–	–
Error	0.15	8	0.0188			1.55
Total	26.71	26				100

SS = Sum of squares; d.o.f = degree of freedom; P = percentage of contribution.

- <sup>a</sup> 99% Confidence.
- <sup>b</sup> 75% Confidence.

### 3.2. Effect of cutting parameters on machining force

Table 4, shows that the feed rate has highest statistical significant (53.38%) followed by depth of cut (36.04%) whereas cutting speed (6.75%) was found to be less

**Table 6**  
ANOVA results for machining power ( $P_m$ ).

Factors	SS	D.o.f	Variance	Test F	$F_{table}$	P (%)
$V_c$	443.93	2	222.00	1219.8	8.65 <sup>a</sup>	77.67
$f$	99.66	2	49.83	273.79	8.65 <sup>a</sup>	17.39
$d$	16.45	2	8.23	45.22	8.65 <sup>a</sup>	2.82
$V_c \times f$	8.94	4	2.24	12.31	7.01 <sup>a</sup>	1.44
$V_c \times d$	0.62	4	0.16	0.88	–	–
$f \times d$	0.07	4	0.018	0.10	–	–
Error	1.45	8	0.182			0.68
Total	571.12	26				100.00

SS = Sum of squares; d.o.f = degree of freedom; P = percentage of contribution.

<sup>a</sup> 99% Confidence.

**Table 7**  
ANOVA results for tool wear ( $VB_{max}$ ).

Factors	SS	D.o.f	Variance	Test F	$F_{table}$	P (%)
$V_c$	372.23	2	186.12	2863.4	8.65 <sup>a</sup>	75.75
$f$	89.95	2	44.98	692.00	8.65 <sup>a</sup>	18.29
$d$	24.48	2	12.24	188.31	8.65 <sup>a</sup>	4.96
$V_c \times f$	2.79	4	0.70	10.77	7.01 <sup>a</sup>	0.52
$V_c \times d$	0.87	4	0.22	3.38	2.81 <sup>b</sup>	0.124
$f \times d$	0.37	4	0.10	1.54	–	0.023
Error	0.52	8	0.065			0.34
Total	491.21	26				100.00

SS = Sum of squares; d.o.f = degree of freedom; P = percentage of contribution.

<sup>a</sup> 99% Confidence.

<sup>b</sup> 90% Confidence.

**Table 8**  
ANOVA results for surface roughness ( $R_a$ ).

Factors	SS	D.o.f	Variance	Test F	$F_{table}$	P (%)
$f$	469.9	2	234.95	978.96	8.65 <sup>a</sup>	83.79
$V_c$	56.91	2	28.45	118.54	8.65 <sup>a</sup>	10.08
$d$	18.53	2	9.27	38.63	8.65 <sup>a</sup>	3.22
$V_c \times d$	5.49	4	1.37	5.71	3.84 <sup>b</sup>	0.81
$f \times d$	4.64	4	1.16	4.83	3.84 <sup>b</sup>	0.66
$V_c \times f$	2.86	4	0.72	3.00	2.81 <sup>c</sup>	0.34
Error	1.90	8	0.24			1.11
Total	560.23	26				100.00

SS = Sum of squares; d.o.f = degree of freedom; P = percentage of contribution.

<sup>a</sup> 99% Confidence.

<sup>b</sup> 95% Confidence.

<sup>c</sup> 90% Confidence.

significant on the machining force. The interactions  $f \times d$  and  $V_c \times f$  were less significant while  $V_c \times d$  interaction was found to be negligible. It can be observed that the increase in machining force caused with the increase in feed rate and depth of cut. But the machining force decreased with increase in cutting speed. The reduction in force was noticed only for the cutting force, while feed force and thrust force remained practically unaltered. The increase in the feed rate induces a larger volume of the cut material in a same unit of time, besides establishing a dynamic effect on the cutting forces. It also leads to corresponding increase in the normal contact stress at the tool chip interface and in the tool chip contact area [7,15]. Hence cutting forces were found to be increased with the

increase in feed rate. Similarly, increase in depth of cut caused the increase in machining forces. It may be due to the fact that, increase in depth of cut results in increased tool work contact length [26]. Subsequently, chip thickness becomes significant that causes the growth of the volume of deformed metal and that requires greater cutting forces to cut the chip. The reduction in the forces with the increase in cutting speed is possibly due to the temperature increase in the shear plane area, which resulted in a reduction in the shear strength of the material [15].

Fig. 4 shows the interaction effects of cutting speed ( $V_c$ ) – feed rate ( $f$ ), cutting speed ( $V_c$ ) – depth of cut ( $d$ ) and feed rate ( $f$ ) – depth of cut on machining force ( $F_m$ ). As seen from Fig. 4a and b, for a given cutting speed, the machining force sharply increases with the increase in feed rate or depth of cut. On the other hand, the machining force has a tendency to reduce with increase in cutting speed with lower feed rate or depth of cut. When the depth of cut is low, the machining force is highly sensitive to feed rate, as shown in Fig. 4c; an increase in feed rate sharply increases the machining force. From the above discussions it can be manifest that, the machining force can be minimized by employing lower values of feed rate and depth of cut with higher cutting speed.

### 3.3. Effect of cutting parameters on specific cutting force

The specific cutting force is highly sensitive to variation of cutting parameters. Table 5, illustrates that the feed rate has highest statistical significant (70.55%) followed by depth of cut (14.05%), whereas cutting speed (13.42%) was found to be less significant on the specific cutting force. The interactions  $f \times d$  was less significant while  $V_c \times f$  and  $V_c \times d$  interaction were found to be negligible. At lower cutting parameters, cutting tool rubs on the surface of work piece in the hard machining, because of not having sufficient material to remove and so the cutting edge undergoes enormous pressure which causes and accelerates its damage or diffusion. The reason might be that at lower cutting parameters, the shear model does not fit adequately to the chip formation process, as the material is subjected to lower strain rates and hence specific cutting force increases. Similar results were reported by Gaitonde et al. [27] during hard turning of AISI D2 steel with ceramic tool.

From the interaction plots Fig. 5a and b it can be observed that, at the low feed rate or depth of cut, an extremely high specific cutting pressure has been recorded. With an increase in feed rate or depth of cut, for a given cutting speed, the specific cutting force decreases. From Fig. 5c illustrates the evolution of the specific cutting force according to the depth of cut and feed rate, specific cutting force decreases with increase in depth of cut and feed rate. It can be concluded that the feed rate exhibits maximum influence on specific cutting force as compared to depth of cut and cutting speed on specific cutting force.

### 3.4. Effect of cutting parameters on machining power

Table 6 presents ANOVA results for machining power. It can be seen that the cutting speed has highest statistical

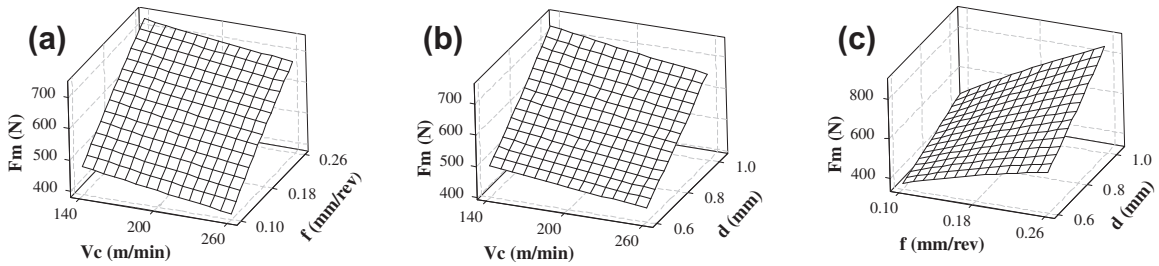


Fig. 4. (a) 3D surface plots for interaction effects of feed rate and cutting speed, (b) depth of cut and cutting speed, and (c) feed rate and depth of cut on machining force.

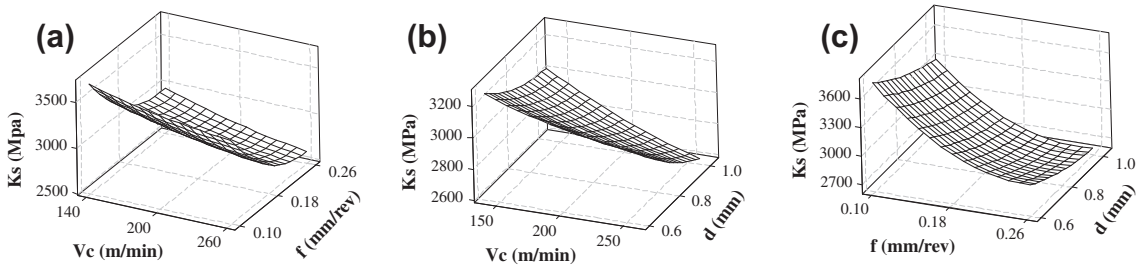


Fig. 5. (a) 3D surface plots for interaction effects of feed rate and cutting speed, (b) depth of cut and cutting speed, and (c) feed and depth of cut on specific cutting force.

significant (77.67%) followed by feed rate (17.39%) and depth of cut (2.82%) on machining power. The interactions  $V_c \times f$  (1.44%) was less significant while  $V_c \times d$  and  $f \times d$  interactions were found to be negligible. It can be observed that at lower cutting parameters, there is a small resistance to cutting tool, and while at the higher cutting parameters, the work material offers more resistance to cutting tool thus increasing the friction. Hence, the cutting force increases due to increase in friction, which in turn increases the power. When the feed rate or depth of cut are increased with the increase of cutting velocities, high power were required to deform the material within short period of time. Similar discussion can be found elsewhere Gaitonde et al. [28,29].

Fig. 6 shows the interaction effects of cutting speed ( $V_c$ ) – feed rate ( $f$ ), cutting speed ( $V_c$ ) – depth of cut ( $d$ ) and feed rate ( $f$ ) – depth of cut on machining power ( $P_m$ ). It can be observed from Fig. 6a and b that, for the given feed rate or depth of cut, the machining power sharply increases with the increase in cutting speed. When the depth

of cut is low, the machining power is highly sensitive to feed rate, as depicted in Fig. 6c; an increase in feed rate slightly increase the machining power. From the above discussion, Fig. 6 clearly suggests that the machining power can be minimized by employing lower values of cutting speed, feed rate and depth of cut.

### 3.5. Effect of cutting parameters on tool wear

The tool wear purely depend on the type of tool grade, geometry, work piece material composition and hardness and cutting conditions. It can be concluded that generally, adhesion, abrasion and diffusion are considered to be the main tool wear mechanisms in hard turning; however the individual effect of each mechanism depends on the work material, cutting conditions and tool geometry [5,30]. From the analysis of Table 7, it indicates that the cutting speed (75.75%) has the highest influence followed by feed rate (18.29%) and depth of cut (4.96%). The interactions  $V_c \times f$  and  $V_c \times d$  were less significant while  $f \times d$

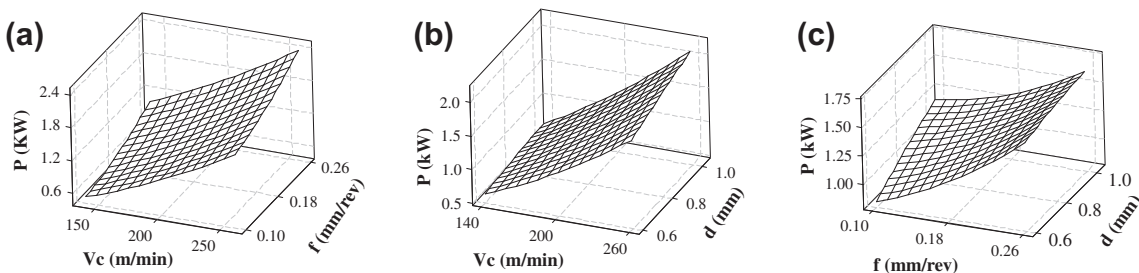
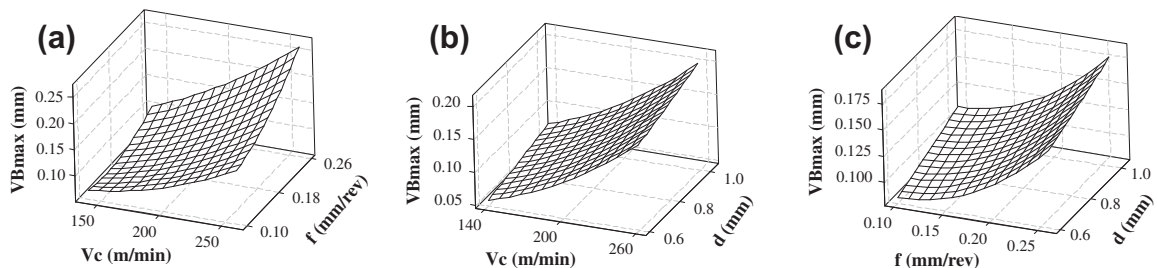


Fig. 6. (a) 3D surface plots for interaction effects of feed rate and cutting speed, (b) depth of cut and cutting speed, and (c) Feed and depth of cut on machining power.

interaction were found to be negligible. From the above discussions it can be observed that, the increased speed significantly increases the temperature at the contact zone, which even exceeds the limits of the allowed thermal stability of the cutting material. Consequently this leads to drastic increase of the tool wear. With simultaneous increase of feed rate and speed of the deformation, the forces, heat generation and consequently the temperature at the contact zone are increased [20,31,32]. With the increase in cutting speed increases 140–260 m/min, the rubbing action between tool and work piece is faster and more heat produced even though less contact time exists. The generation of heat at the flank side softens the tool edge and more wear occurred.

From the interaction plots Fig. 7a and b, it can be observed that, for the given feed rate or depth of cut, the cutting tool wear increases with the increase in cutting speed. On the other hand, the tool wear has a tendency to reduce with increase in feed rate and depth of cut with low cutting speed. Fig. 7c indicates the characteristic wear of tool is caused by the fact that, the speed is no longer the influential factor on wear, but it is more likely that wear is the consequence of the feed and depth of cut. From the above discussions, it is clear that a combination of lower values of cutting speed, feed rate and depth of cut is favorable in reducing tool wear.



**Fig. 7.** (a) 3D surface plots for interaction effects of feed rate and cutting speed, (b) depth of cut and cutting speed, and (c) feed and depth of cut on tool wear.

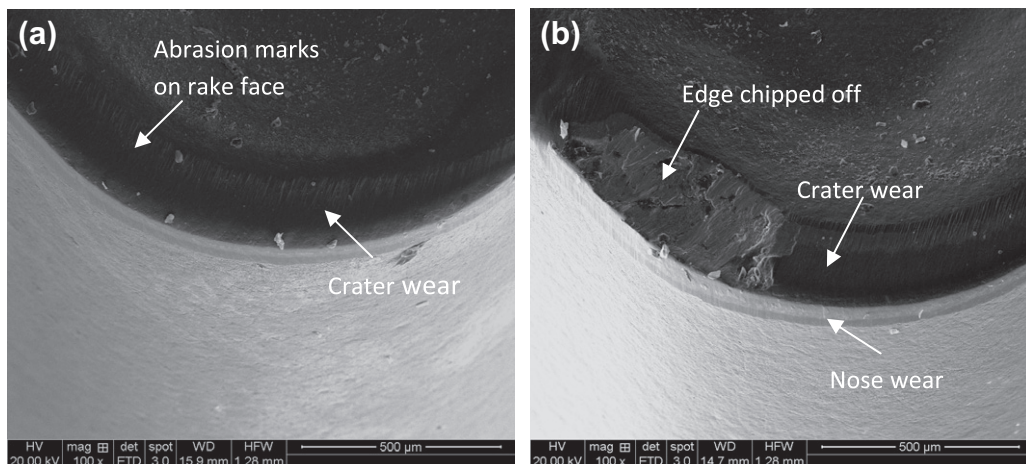


**Fig. 8.** (a) Crater wear on the rake face of the tool at the cutting condition  $V_c = 200$  m/min,  $f = 0.10$  mm/rev and  $d = 0.6$  mm. (b) Chipping of cutting edge at  $V_c = 260$  m/min,  $f = 0.26$  mm/rev and  $d = 0.8$  mm.

Fig. 8 shows the wear of the multilayer coated carbide cutting tool observed with the scanning electronic microscopy (SEM) after the machining tests. The formation of wear is due to the occurrence of higher pressure and temperature at the tool. The results of the present study also agree with the study of Davim and Figueira [12] during hard turning of AISI D2 steel.

Fig. 8a shows that, while flank wear progress is steadier, the crater formation on the rake face is highly influenced by thermal conditions and associated chemical wear. It can be concluded that the increase in tool wear at higher values of cutting speed is probably due to the abrasion at the rake face of the tool as the machining time progresses. According to Thanizhmanii et al. [33], during hard turning with PCBN tools distinct wear mechanisms may coexist, chiefly abrasion and adhesion. However, in the case of hard turning with carbide tools, their comparatively lower hardness makes abrasion the dominant wear mechanism. The film is removed from the region near the cutting edge after short period and the substrate is exposed. It may be due to the fact that hardness reduction and increase of thermal conductivity of the coating at the elevated cutting temperature [34]. In spite of that, there is no significant increase in the wear extension on the rake face, suggesting that the coating removal is ruled by critical shear stress and temperature values in the flow zone. Excessive crater wear

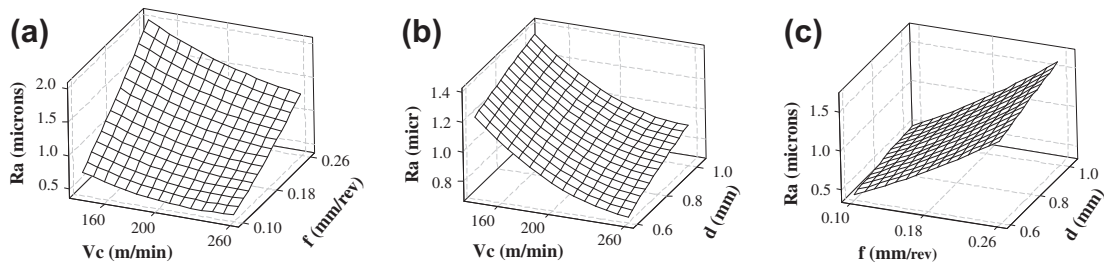


**Fig. 9.** (a) 3D surface plots for interaction effects of feed rate and cutting speed, (b) depth of cut and cutting speed, and (c) feed and depth of cut on surface roughness.

weakens the cutting edge and causes a catastrophic failure (chipping) of the tool as shown in Fig. 8b. The fracture observed may be due to the extremely high shear stresses generated by the steep temperature gradient experienced by the tool as a result of cutting the hardened steel. Deformation of the cutting edge usually occurs at high feed rates and high cutting speeds since the hardness of the tool decreases with increasing cutting speed.

### 3.6. Effect of cutting parameters on surface roughness

Surface roughness influences not only dimensional accuracy of machined parts but also their properties. Surface roughness is an important parameter to evaluate the performance of the cutting tools. The irregularity of a machined surface is the result of the machining process, including selection of cutting conditions, environmental conditions. In hard turning process, the surface roughness is greatly affected by a number of factors such as nose radius, work hardness, cutting angles and cutting conditions. Table 8 indicates that all the factors have significant influence on the variation of surface roughness. The percent contribution indicates that the feed rate factor (83.79%), cutting speed factor (10.08%) and depth of cut factor (3.22%) have great influence on the surface roughness. It can be revealed that lower surface roughness values are obtained at higher cutting speeds due to lower forces generated. At high cutting speed, better surface finish was obtained since less heat was dissipated to the work material.

The amount of heat generation increases with increase in feed rate, because the cutting tool has to remove more volume of material from the work piece. The plastic deformation of the work piece is proportional to the amount of heat generation in the work piece and promotes roughness on the work piece surface [35–37]. And the second point is that cutting with coated carbide tool having a certain wear generates surface roughness than a fresh tool, because the tool wear is proportional to the cutting feed rate and roughness is a reproduction of the tool nose profile on the work piece surface [22]. Depth of cut parameter has a very less effect compared to that of the feed rate. This is due to the increased length of contact between the tool and the work piece. This improves the conditions of heat flow from the cutting zone and consequently slows down the process wear.

From interaction plot Fig. 9a it can be observed that, for a given cutting speed, the surface roughness sharply

increases with increase in feed rate. On the other hand, surface roughness has a tendency to reduce with an increase in cutting speed at constant feed rate. The minimal surface roughness results with the combination of low feed rate and high cutting speed. Fig. 9b indicates that the depth of cut is low; the surface roughness is highly sensitive to cutting speed; an increase in cutting speed sharply reduces the surface roughness. However, this reduction becomes smaller and smaller with higher values of depth of cut. Usually depth of cut does not much influence the surface roughness. Fig. 9c indicates that for a given depth of cut, the surface roughness increases with increase in feed rate. On the other hand, depth of cut has less effect on surface roughness. It revealed that a combination of higher cutting speed along with lower feed rate and depth of cut is necessary for minimizing the surface roughness. Best surface finish of  $0.32 \mu\text{m}$  was recorded at higher cutting speed of 260 m/min, feed rate of 0.1 mm/rev and depth of cut of 0.6 mm. Fig. 10 shows the scanning electron microscopy (SEM) image in the quality of the surface observed during turning of AISI 4340 high strength low alloy steel using coated carbide tool at the cutting conditions of cutting speed of 260 m/min, feed rate of 0.1 mm/rev, depth of cuts of 1.0 mm and a machining time of 4 min. The improved surface finish is clearly evidenced in this figure for reduced feed rate.

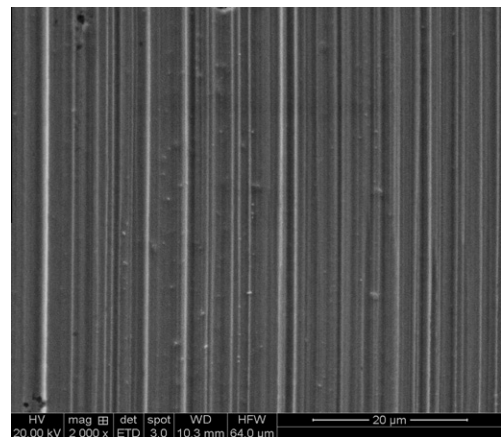


**Fig. 10.** SEM view of machined surface generated at  $V_c = 260$  m/min,  $f = 0.10$  mm/rev and  $d = 1.0$  mm.

3.7. Correlations

The correlation between the cutting factors and measured machining force, power, specific cutting force, tool wear and surface roughness are determined from the following multiple linear regression equations (Eqs. (4)–(8)). The coefficients of determination ( $R^2$ ) values of developed machinability models have very good correlations between the experimental and predicted values of machinability characteristics.

The Anderson–Darling test and normal probability plots of the residuals versus the predicted response for the machining force, specific cutting force, machining power, tool wear and surface roughness are plotted in Figs. 11–15. The data closely follows the straight line. The null hypothesis is that the data distribution law is normal and the alternative hypothesis is that it is non-normal. Using the  $p$  value which is greater than alpha of 0.05 (level of significance), the null hypothesis cannot be rejected (i.e., the data follow a normal distribution). It implies that the models proposed are adequate.

$$F_m = 124 + 0.653V_c + 18f + 248d - 3.41V_c \times f - 1.05V_c \times d + 2885f \times d, \quad (R^2 = 97.5\%) \quad (4)$$

$$K_s = 5301 - 2.05V_c - 5565f - 1208d - 3.44V_c \times f - 0.06V_c \times d + 2161f \times d, \quad (R^2 = 93.3\%) \quad (5)$$

$$P_m = -0.138 + 0.00350V_c - 2.15f - 1.21d + 0.0168V_c \times f + 0.00649V_c \times d + 3.67f \times d, \quad (R^2 = 98.0\%) \quad (6)$$

$$VB_{max} = 0.0330 + 0.000018V_c c - 0.610f - 0.0785d + 0.00389V_c \times f + 0.000514V_c \times d + 0.344f \times d, \quad (R^2 = 95.7\%) \quad (7)$$

$$R_a = 0.166 - 0.00427V_c + 10.9f - 0.357d - 0.0158V_c \times f + 0.00472V_c \times d - 0.89f \times d, \quad (R^2 = 97.3\%) \quad (8)$$

3.8. Confirmation tests

For the validation purpose, the experiments were conducted for three new trials, consisting of combination of

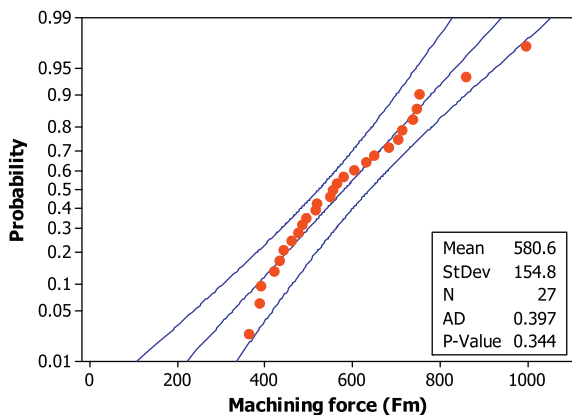


Fig. 11. Normal probability plots of machining force.

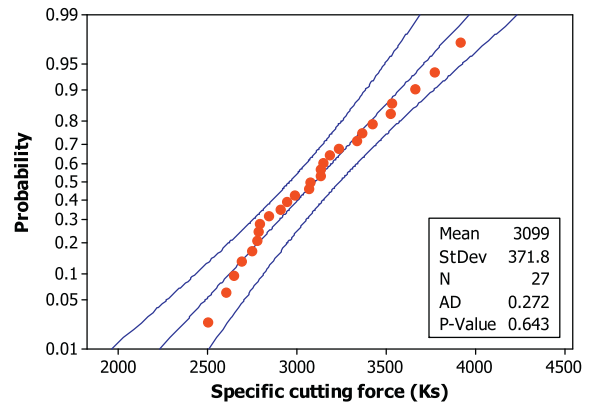


Fig. 12. Normal probability plots of specific cutting force.

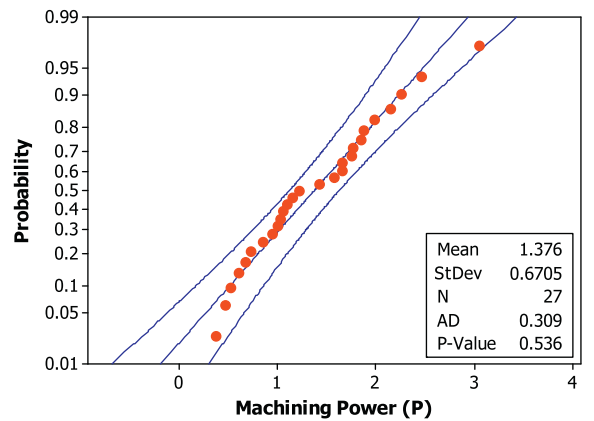


Fig. 13. Normal probability plots of machining power.

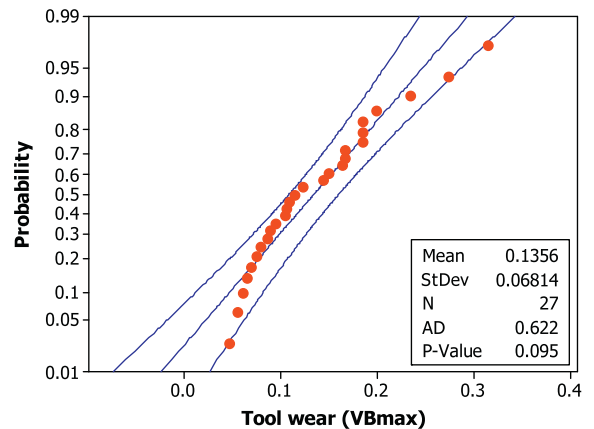


Fig. 14. Normal probability plots of tool wear.

input process parameters, which do not belong to the plan of experimental set. The machining parameters used for confirmation tests are illustrated in Table 9.

Table 10 shows the results obtained where a comparison was done between the foreseen values from the model developed in the present work (Eqs. (4)–(8)); with the val-

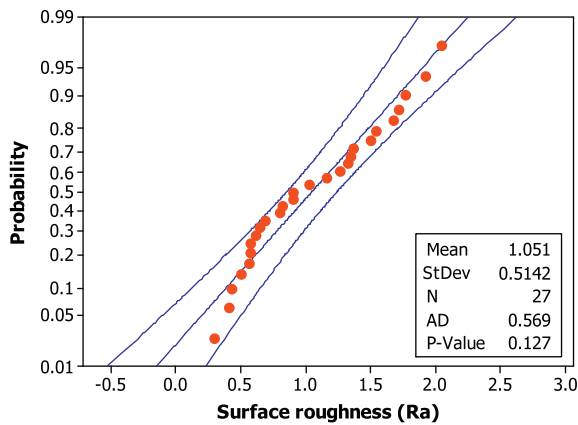


Fig. 15. Normal probability plots of surface roughness.

Table 9

Cutting parameters used in turning conformations tests.

Test	$V_c$ (m/min)	$f$ (mm/rev)	$d$ (mm)
1c	160	0.12	0.65
2c	190	0.16	0.75
3c	230	0.24	0.95

Table 10

Comparison of results obtained from experiment with model.

Sl. No	Test	Experiment	Model (Eqs. )(4)–(8)	Error (%)
1. Machining force ( $F_m$ ) in N				
	1c	444.20	456.50	2.77
	2c	529.86	516.13	2.59
	3c	754.23	783.81	3.93
2. Specific cutting force ( $K_s$ ) in MPa				
	1c	3616.3	3575.2	1.14
	2c	3262.0	3178.9	2.55
	3c	2636.0	2560.57	2.86
3. Machining power ( $P_m$ ) in kW				
	1c	0.661	0.70	5.90
	2c	1.152	1.23	6.77
	3c	2.184	2.24	2.56
4. Tool wear ( $VB_{max}$ ) in mm				
	1c	0.0667	0.070	4.95
	2c	0.1128	0.115	1.95
	3c	0.2216	0.232	4.69
5. Surface roughness ( $R_a$ ) in $\mu$				
	1c	0.68	0.72	5.88
	2c	0.92	0.96	4.35
	3c	1.42	1.48	4.23

ues obtained experimentally. From the analysis of Table 10, we can observe that the calculated error for machining force ( $F_m$ ) (max. value 3.93% and min. 2.59%), specific cutting force ( $K_s$ ) (max. value 2.86% and min. 1.14%), machining power ( $P_m$ ) (max. value 6.770% and min. 2.54%), tool wear ( $VB_{max}$ ) (max. value 4.95% and min. 1.95%) and surface roughness ( $R_a$ ) (max. value 5.88% and min. 4.23%). Therefore, Eqs. (4)–(8) correlate the relationship of the machining force, power, specific cutting force, tool wear and surface roughness with the cutting parameters with reasonable degrees of approximation.

## 4. Conclusions

The following conclusions can be drawn from this investigation on turning of hardened AISI 4340 steel using coated carbide at different cutting parameters:

- The feed rate has highest physical as well statistical influence on the machining operation (53.38%) followed by depth of cut (36.04%) and cutting speed (6.75%). Machining force initially increases with increase in feed rate and depth of cut and decreases with increase in cutting speed. The reduction in the forces is probably due to temperature increase in the shear plane area, resulted in a reduction in shear strength of the material.
- The feed rate has highest influence on the specific cutting force to perform the machining operation (70.55%) followed by depth of cut (14.05%) and cutting speed (13.42%). At lower feed rate, shear of material does not fit adequately to the chip formation process. As the material is subjected to lower strain rates, it leads to an increase in the specific cutting force.
- The cutting speed has the highest influence on the machining power required to perform machining operation (77.67%) followed by feed rate (17.39%) and depth of cut (2.82%). When the cutting speed increases with feed rate and depth of cut, higher power is required for the deformation of material within short period of time.
- The cutting speed has highest influence on the tool wear (75.75%) and feed rate (18.29%) and then depth of cut (4.96%). In hard machining, increased cutting speed significantly increases the temperature at the contact zone, consequently resulting in drastic increase of the tool wear.
- The feed rate has highest influence on surface roughness (83.79%), cutting speed (10.08%), and followed by depth of cut (3.99%). The surface finish was improved as cutting speed was increased and deteriorated with feed rate. The optimum parameter setting for better surface finish is obtained at a higher cutting speed with low feed rate.
- The multiple regressions were obtained to predict the cutting forces, machining power, tool wear and surface roughness. The models were validated through confirmation tests.

## Acknowledgments

The authors are grateful to Kennametal India Ltd., Bangalore for providing facilities to conduct experiments and support throughout this work.

## References

- [1] G. Byrne, D. Dornfeld, B. Denkena, Advancing cutting technology, Ann. CIRP 52 (2) (2003) 483–507.
- [2] J.S. Dureja, V.K. Gupta, V.S. Sharma, M. Dogra, Wear mechanisms of TiN-coated CBN tool during finish hard turning of hot tool die steel, Proc. IMechE Part B: J. Eng. Manuf. 224 (2010) 553–566.

- [3] M. Aneiro Federico, T. Coelho Reginaldo, C. Brandao Lincoln, Turning hardened steel using coated carbide at high cutting speeds, *J. Brazil Soc. Mech. Sci. Eng.* 30 (2) (2008) 104–109.
- [4] K. Nakayama, M. Arai, T. Kanda, Machining characteristics of hard materials, *Ann. CIRP* 37 (1) (1998) 89–92.
- [5] S.Y. Luo, Y.S. Liao, Y.Y. Tsai, Wear characteristics in turning high hardened alloy steels by ceramic and CBN tools, *J. Mater. Process. Technol.* 88 (1999) 114–121.
- [6] J.A. Arsecularatne, L.C. Zhang, C. Montross, P. Mathew, On machining of hardened AISI D2 steel with PCBN tools, *J. Mater. Process. Technol.* 171 (2) (2006) 244–252.
- [7] M.A. Yallese, K. Chaoui, N. Zeghib, L. Boulanouar, Hard machining of hardened bearing steel using cubic boron nitride tool, *J. Mater. Process. Technol.* 209 (2009) 1092–1104.
- [8] Qian Li, Hossan Mohammad Robiul, Effect on cutting force in turning hardened tool steels with cubic boron nitride inserts, *J. Mater. Process. Technol.* 191 (1–3) (2007) 274–278.
- [9] T. Ozel, Karpat Yigit, Predictive modeling of surface roughness and tool flank wear in hard turning using regression and neural net works, *J. Mater. Process. Technol.* 45 (2005) 467–479.
- [10] Y.K. Chou, H. Song, Tool nose radius effects on finish hard turning, *J. Mater. Process. Technol.* 148 (2004) 259–268.
- [11] W.H. Yang, Y.S. Tarn, Design optimization of cutting parameters for turning operations based on the Taguchi method, *J. Mater. Process. Technol.* 84 (1998) 122–129.
- [12] J.P. Davim, L. Figueira, Comparative evaluation of conventional and wiper ceramic tools on cutting forces, surface roughness, and tool wear in hard turning AISI D2 steel, *J. Eng. Manuf.* 221 (2007) 625–633.
- [13] T. Ozel, T.K. Hsu, E. Zeren, Effects of cutting edge geometry, workpiece hardness, feed rate and cutting speed on surface roughness and forces in finish turning of hardened AISI H13 steel, *Int. J. Adv. Manuf. Technol.* 25 (2007) 262–269.
- [14] Y. Sahin, A.R. Motorcu, Surface roughness model for machining mild steel with coated carbide tool, *Mater. Des.* 26 (4) (2005) 321–326.
- [15] J.G. Lima, R.F. Avila, A.M. Abrao, M. Faustino, J.P. Davim, Hard turning: AISI 4340 high strength low alloy steel and AISI D2 cold work tool steel, *J. Mater. Process. Technol.* 169 (2005) 388–395.
- [16] R. Yigit, Celik Erdal, Findik Fehim, Koksak Sakip, Tool life performance of multilayer hard coatings produced by HTCVD for machining of nodular cast iron, *Int. J. Refract. Met. Hard Mater.* 26 (2008) 514–524.
- [17] F.M. Aneiro, Reginaldo T. Coelho, Lincoln C. Brandao, Turning hardened steel using coated carbide at high cutting speeds, *J. Brazil Soc. Mech. Sci. Eng.* 30 (2) (2008) 104–109.
- [18] A. Knutsson, M.P. Johansson, L. Karlsson, M. Oden, Machining performance and decomposition of TiAlN/TiN multilayer coated metal cutting inserts, *J. Surf. Coat. Technol.* 205 (2011) 4005–4010.
- [19] R. Yigit, Celik Erdal, Findik Fehim, Performance of multilayer coated carbide tools when turning cast iron, *Turk. J. Eng. Environ. Sci.* 33 (2009) 147–157.
- [20] I. Ciftci, Machining of austenitic stainless steels using CVD multilayer coated cemented carbide tools, *Trib. Int.* 39 (2006) 565–569.
- [21] K.D. Bouzakis, S. Hadjiyiannis, G. Skordaris, The influence of the coating thickness on its strength properties and on the milling performance of PVD coated inserts, *Surf. Coat. Technol.* 175 (2003) 393–401.
- [22] Axinite, R.C. Dewes, Surface integrity of hot work tool steel after speed milling-experimental data and empirical model, *J. Mater. Process. Technol.* 127 (2002) 325–335.
- [23] A.E. Diniz, A.J. De Oliveira, Optimizing the use of dry cutting in rough turning steel operations, *Int. J. Mach. Tools Manuf.* 44 (2004) 1061–1067.
- [24] J.P. Davim, Design of optimization of cutting parameters for turning metal matrix composites based on the orthogonal arrays, *J. Mater. Process. Technol.* 132 (2003) 340–344.
- [25] J.A. Ghani, I.A. Choudhury, H.H. Hassan, Application of Taguchi method in the optimization of end milling parameters, *J. Mater. Process. Technol.* 145 (2004) 84–92.
- [26] H. Bouchelaghem, M.A. Yallese, T. Mabrouki, A. Amirat, J.F. Rigal, Experimental investigation and performance analyses of CBN insert in hard turning of cold work tool steel (D3), *Mach. Sci. Technol.* 14 (2010) 471–501.
- [27] V.N. Gaitonde, S.R. Karnik, L. Figueira, J.P. Davim, Performance comparison of conventional and wiper ceramic inserts in hard turning through artificial neural network modeling, *Int. J. Adv. Manuf. Technol.* 52 (2011) 101–114.
- [28] V.N. Gaitonde, S.R. Karnik, L. Figueira, J.P. Davim, Machinability investigations in hard turning of AISI D2 cold work tool steel with conventional and wiper ceramic inserts, *Int. J. Refract. Met. Hard Mater.* 27 (4) (2009) 754–763.
- [29] V.N. Gaitonde, S.R. Karnik, L. Figueira, J.P. Davim, Analysis of machinability during hard turning of cold work tool steel (type: AISI D2), *Mater. Manuf. Process.* 24 (12) (2009) 1373–1382.
- [30] S. Dolisnk, J. Kopac, Mechanism and type of tool wear: particularly in advanced cutting tool materials, *J. Achieve Mater. Manuf. Eng.* 19 (1) (2006) 11–18.
- [31] Y. Isik, Investigating the machinability of tool steels in turning operation, *Mater. Des.* 28 (5) (2007) 1417–1424.
- [32] R. Quiza, L. Figueira, J.P. Davim, Comparing statistical models and artificial neural networks on predicting the tool wear in hard machining D2 AISI steel, *Int. J. Adv. Manuf. Technol.* 37 (2008) 641–648.
- [33] S. Thamizhmanii, K. Kamarudin, E.A. Rahim, A. Sapparudin, S. Hassan, Tool wear and surface roughness in turning AISI 8620 using coated ceramic tool, In: *Proceedings of the world congress on engineering-2 (WCE -2007)*, London, UK, 2007.
- [34] T. Childs, K. Maekawa, T. Obikawa, Y. Yamane, *Metal Machining: Theory and Applications*, Edward Arnold, London, 2000.
- [35] J.P. Davim (Ed.), *Machining of Hard Materials*, Springer, 2011.
- [36] J.D. Thiele, S.N. Melkote, Effect of cutting edge geometry and work piece hardness on surface generation in the finish hard turning of AISI 52100 steel, *J. Mater. Process. Technol.* 94 (1999) 216–226.
- [37] J.A. Arsecularatne, L.C. Zang, C. Montross, P. Mathew, On machining of hardened AISI D2 steel with PCBN tools, *J. Mater. Process. Technol.* 171 (2006) 244–252.